Stony Brook University

Investigation of a New Pathway Toward a Viable High-Field MgB_2 Conductor by Plasma Spray Synthesis of a Carbon-Doped Boron Precursor

A Thesis Presented

by

Paul Stephen Chang

to

The Graduate School

in Partial Fulfillment of the

Requirements

for the Degree of

Master of Science

in

Materials Science and Engineering

Stony Brook University

December 2008

Stony Brook University

The Graduate School

Paul Stephen Chang

We the thesis committee for the above candidate for the

Master of Science degree, hereby recommend

acceptance of this thesis.

David Welch, PhD – Thesis Advisor
Adjunct Professor, Materials Science and Engineering

Sanjay Sampath, PhD – Chairperson of Defense
Professor, Materials Science and Engineering

Lance Cooley, PhD
Scientist, Fermi National Accelerator Laboratory

This thesis is accepted by the graduate school.

Lawrence Martin
Dean of the Graduate School

Abstract of the Thesis

Investigation of a New Pathway Toward a Viable High-Field MgB_2 Conductor by Plasma Spray Synthesis of a Carbon-Doped Boron Precursor

by

Paul Stephen Chang

Master of Science

in

Materials Science and Engineering

Stony Brook University

2008

The use of superconducting MgB_2, which has a T_c ~40 K, in engineering applications will reduce costs associated with the use of cryogenic liquid He that is necessary with current technology and will improve design options for devices like patient-friendly open MRI systems. The main obstacle to achieving this is the poor high-field performance of this multiband superconductor. This thesis explores a new pathway toward a viable high-field MgB_2 conductor. The method presented utilizes plasma spray to synthesize a nanoscale boron carbide powder from gas phase precursors. This enables the integration of the important alloying element (carbon) on an atomic scale. This is different than all other routes to date, which either add boron and carbon separately and therefore require diffusion at excessive temperatures for wire technology, or use high energy milling to create an atomic boron-carbon mixture which incorporates high amounts of disorder. This thesis shows that the plasma-sprayed boron carbide produces a uniformly alloyed MgB_2 that is relatively free from defects and can be reacted at temperatures low enough for making wires.

Table of Contents

List of Figures

List of Tables

Acknowledgements

I would like to thank my advisors, Lance Cooley and David Welch for giving me immense support and motivation throughout this project and for their valuable teachings on superconductivity. I must also thank Sanjay Sampath for his support of this thesis work and the use of facilities at the Center for Thermal Spray Research (CTSR). Also from CTSR, I would like to thank Glenn Bancke for providing me with the plasma sprayed powder that is central to this work. Jim Marzik at Specialty Materials, Inc. also deserves my appreciation for the powder synthesis. I would like to extend my gratitude to Arnold Moodenbaugh for his help with x-ray diffraction and the Brookhaven National Laboratory for the use of their facilities. I am deeply indebted to the David Larbalestier and Jian Zhou at the National High Magnetic Field Laboratory at Florida State University for all the resistivity measurements. This work was supported by the MRSEC program of the National Science Foundation (Supplemented by NSF Division of Physics) and by the Stony Brook-BNL Seed Grant Program. Lastly, I would like to say a special thank you to my wife and family for the love and support that they give me always.

1. Magnesium Diboride (MgB_2)

The January 2001 discovery of superconductivity in magnesium diboride at 39K [1] was a historical moment in this field. The surprisingly high T_c for a binary compound with a simple hexagonal structure generated a large amount of excitement and this discovery was followed by a flurry of activity. Within seven months, over 260 studies on this material had emerged [2]. The general enthusiasm also led to the discovery of other superconductors, especially in materials related to MgB_2 [3-6] as well as in elemental boron under pressure [7]. The T_c of MgB_2 is higher than the most widely used superconductors NbTi ($T_c \sim 9K$) and Nb_3Sn ($T_c \sim 18K$). Although its T_c is about three times lower than that of the high-T_c superconducting (HTSC) cuprates [8], these cuprates require complex manufacturing and the cost of making wires is high. MgB_2 carries critical current densities similar to these competing materials and is relatively cheap and simple to manufacture. These factors combined with its high transition temperature make it a contender for the preferred material in many superconductor applications. MgB_2 powder has been commercially available since early 1950s and it also can be made into thin films [9-14], single crystals [15-18], wires [19-22] and tapes [9, 21, 23]. These available fabrication methods enabled the study of MgB_2 for applications. Several commercial applications are imminent in the 20-30K and 1-4T range, but for uses in high fields more improvements need to be made. The most prominent potential application is open MRI systems with MgB_2 magnets that operate without liquid cryogens. Prototypes of these MRI devices have been made and tested [20, 24-26]. Details of MRI and other applications in refrigeration, fault current limiters, transformers, motors, generators, adiabatic demagnetization refrigerators, superconducting magnetic energy storage, and high-energy physics are presented by Tomsic et al [27].

The interest in MgB_2 is not only due to its potential for industrial applications and cheap raw materials, but also for fundamental scientific research. MgB_2 has a simple hexagonal crystal structure with spacegroup p6/mmm. The MgB_2 structure is shown in Figure 1. The boron forms graphite-like layers separated by close-packed hexagonal layers of magnesium. The magnesium atoms line up with the center of the hexagons formed by boron and the in-plane B-B lengths are much shorter than the inter-plane lengths. The electronic states at the Fermi level consist primarily of the σ and π boron bonds. A full description of the electronic and crystal structure is given

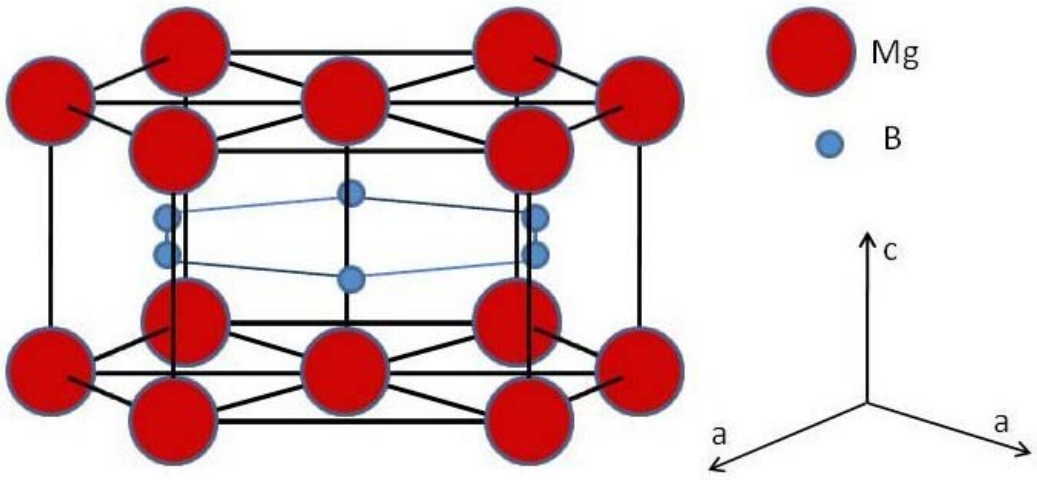

Figure 1.1 The crystal structure of magnesium diboride.

by Ivanovskii [28]. The high T_c found in this material is surprising because of this simple structure. An interesting finding is the existence of multiple superconducting band gaps[29] which was predicted by various researchers [30-32]. The σ states confined to the boron plane couple strongly with the lattice vibrations and create a large superconducting band gap. The π states couple weakly with phonons to create a much smaller band gap. At 17K the σ band is 6.5eV and the π band is 1.5eV. Due to coupling, both gaps develop at the same T_c. The BCS description of superconductivity [33] leads to the prediction that low-mass elements would have higher T_c because of higher frequency phonon modes. Predictions have been made for hydrogen to have the highest T_c for a monatomic superconductor [34]. The discovery of superconductivity in MgB_2 gave credence to these predictions because of the strong contribution of the boron layers [31, 32, 35]. MgB_2 indeed showed signs of the familiar phonon mediated superconductivity as outlined by BCS when samples made from the isotopes B-11 and B-10 were found to have a 1K difference in T_c [36]. This variation of T_c with atomic mass is known as the isotope effect and is discussed further in section 2.

The widespread use of MgB_2 still depends on increasing its upper critical field, H_{c2} i.e. the value of the applied magnetic field at which superconductivity disappears. This can be achieved by adding non-magnetic impurities and other disorder producing means. This work is a study of a novel method for preparing carbon doped MgB_2 in an attempt to produce a homogeneously doped material with an increased upper critical field. The results have implications for both applications

and pure science. The next section will describe the nature of superconductivity in MgB_2 followed by a review of the methods of fabricating doped samples and the resulting superconducting parameters.

2. Superconductivity and properties of MgB_2

2.1. General Superconductivity

Superconductivity was discovered by Kamerlingh Onnes in 1911. He conducted extensive research in cryogenics and was the first to liquefy helium at 4.2K. What he observed was that the electric resistance of mercury dropped drastically at about 4 K below which it was immeasurably low. Onnes described this as a newly discovered state of the material which he called the "superconducting state" which occurs at and below the critical temperature T_c. He predicted that this state would be used to produce superconducting magnets with fields exceeding 10T. First attempts at these magnets were not successful due to the loss of superconductivity with small applied fields and Onnes' prediction did not come true until many years later.

In 1933, Meissner and Oschenfeld discovered perfect diamagnetism in superconductors. What they found was that an applied field was excluded from a superconductor as well as from an originally normal material when it is cooled below T_c. If superconductivity were explained by simply zero resistance then the flux penetrating the normal material would be trapped after the transition. This feature of superconductivity is known as the Meissner effect. In order to exclude flux in this way, a superconductor develops a shielding current at its surface which creates a field that cancels the applied field. This current flows within a short depth of the surface known as the penetration depth λ. The shielding current increases as the applied field is increased until the required shielding current density reaches a limiting value above which superconductivity cannot be sustained, i.e. the depairing current J_d. The energy of J_d is equal to the energy gap of the superconducting state. The field that induces J_d is known as the thermodynamic critical field H_c.

The next important breakthrough in superconductivity was the discovery of a second class of superconductors which we now call type-II. This class of superconductor could sustain high current densities even in high fields. The cutoff field for superconductivity in type-II materials (H_{c2}) is much higher than H_c of the type-II materials and thus engineering applications almost exclusively use type-II materials.

Abrikosov made significant contributions to understanding of type-II superconductivity using the phenomenological Ginzburg-Landau (GL) theory. The

surface energy E_s between normal and superconducting regions is

$$E_s = \frac{1}{2}\mu_0 H_c^2(\xi - \lambda) \qquad \text{Eq 2.1}$$

where ξ is the coherence length over which the superconductivity order parameter decays and is effectively the thickness of the boundary between the two regions. The GL parameter $\kappa = \lambda/\xi$ and Abrikosov showed that the value of κ determined if a material was type-I or type-II. Namely, for type-I materials $\kappa < 1/\sqrt{2}$ and for type-II materials $\kappa > 1/\sqrt{2}$. He found that in the latter case this leads to a gradual increase in magnetic flux penetration by quantized increments beginning at a lower critical field H_{c1}. For field between H_{c1} and H_{c2} the penetrating flux is contained in normal cores of radius ξ which are distributed within the superconducting matrix. Furthermore, the flux in each core is a quantized amount called a fluxon ϕ_0 given in terms of the universal constants h (Planck's constant), c (the speed of light in a vacuum), and e (the electronic charge) by

$$\Phi_0 = \frac{\mathrm{hc}}{2\mathrm{e}} = 2.07 \times 10^{-7}\mathrm{gauss} - \mathrm{cm}^2 \qquad \text{Eq 2.2}$$

Each core is surrounded by a vortex of circulating supercurrent which shields the superconducting region from the flux. This system of normal flux-carrying cores within superconducting material is known as the mixed state or Abrikosov vortex state. The quantized flux penetration lowers the energy of holding the field out which explains why H_{c2} can be much greater than H_c.

The distribution of fluxons in a perfect superconductor is controlled by the mutual repulsion on each other. This results in a close packed hexagonal array called a flux line lattice (FLL). As the applied field is increased more fluxons are forced into the sample decreasing the spacing of the FLL until at H_{c2} they overlap and the entire material loses superconductivity. H_{c1} and H_{c2} are defined by the following

$$H_{c1} = \frac{H_c}{\kappa} \qquad \text{Eq 2.3}$$

$$H_{c2} = \sqrt{2}\kappa H_c = \frac{\Phi_0}{2\pi\xi^2} \qquad \text{Eq 2.4}$$

Current flowing through a type-II superconductor exerts a Lorentz force ($\mathbf{F}_L = \mathbf{J} \times \mathbf{B}$) on the fluxons. This cause sideways motion of the flux lines which induces a "resistive" voltage. The imperfections and impurities present in real materials lower

the free energy of the superconductor when they are present within the fluxons and act as pinning sites. The critical current density is then reached when F_L is equal to the flux pinning force F_P. So if F_L is greater than F_P the fluxons move and the material shows a finite resistance.

The microscopic theory of Bardeen, Cooper and Schreiffer (BCS) [33] describes the framework in which superconductivity works. In 1956 L.N. Cooper presented the idea that a weak attraction between them could cause electrons to bind into pairs [37]. Cooper showed that at adequately low temperatures the Fermi electrons are unstable against the formation of the bound pair. These Cooper pairs have zero net spin and zero net linear momentum. Thus as a pair they do not obey Fermi-Dirac statistics which allows them to condense into the lowest energy state with a single coherent wavefunction ψ. This wavefunction continues over the entire sample and forms a coherent system which defines superconductivity. Usually, electrons repel each other because of Coulombic forces so this pairing mechanism must include additional interactions. In the BCS description the interaction is initiated when the first electron attracts the positively charged ions and causes a charge polarization. The increase in positive charge then attracts another electron creating an attractive interaction, described as being mediated by a phonon, between the two electrons which can overcome the Coulombic repulsive forces. At sufficiently low temperatures the random thermal vibrations are not strong enough to affect this interaction and the Cooper pairs described above are created. Soon after the BCS paper, calculations done by Pines[38] showed that the phonon mediated interaction is of the same order as the direct Coulomb repulsion thus showing that a net attractive interaction due to phonon mediation is a realistic result.

2.2. Superconductivity in MgB_2

One of the foremost questions about MgB_2 was whether the microscopic interactions were similar to that in the low T_c metallic superconductors. Since its transition temperature was higher than all the usual phonon mediated superconductors, it was speculated that there might be some type of exotic coupling in MgB_2. The BCS theory is based upon the interaction between electrons and lattice vibrations. Thus it is reasonable to assume that the mass of the element M would have an effect on the transition temperature of a superconductor due to its effect on the characteristic phonon frequency of the lattice. This was confirmed by the discovery of the isotope effect[39, 40]. The isotope effect gives a correlation between

T_c and the mass of the element M. The relationship is defined by the isotope coefficient α, where

$$\alpha = -\frac{d \ln T_c}{d \ln M} \qquad \text{Eq 2.5}$$

for a single-element system and

$$\alpha = \sum_i \alpha_i = \sum_i -\frac{\partial \ln T_c}{\partial \ln M_i} \qquad \text{Eq 2.6}$$

for a multielement system. In the case of a moderately coupled classical BCS superconductors the value of α is 0.5. The isotope effect has largely been used to identify the nature of superconductivity in a material. The boron isotope effect was found in MgB_2 [36] with α(B) = 0.25 and later studies showed α(B) = 0.30 and α(Mg) = 0.02 [41, 42]. This confirms that BCS electron-phonon interaction is involved in the superconductivity of MgB_2. However, some questions still arise because the isotope coefficient found in MgB_2 is significantly lower than the expected 0.5. A few factors have been proposed as the cause of this reduced α including the Coulomb repulsion between paired electrons, the two-band nature of MgB_2 and the anharmonic character of the phonon spectrum. In most of these cases the studies have shown that the measured α is too low to be accounted for by the proposed factors and a definitive explanation is still sought[41]. In MgB_2, two-dimensional σ-bands develop from the boron p_{xy} orbitals and three-dimensional π-bands develop from the boron p_z orbitals. The σ bands couple strongly to the boron in-plane phonon modes and produce superconductivity. The π-bands couple weakly and become superconductive with a much smaller energy gap.

2.3. Comparison of modern superconductors

There are hundreds of known superconductors but only a few are commercially applicable and compete with MgB_2. This is because real engineering uses, such as magnets, require that the superconductor be formed into a long wire with an electrical stabilizer, fine filaments, insulation, and other features, in addition

to having strong superconductivity. The vast majority of superconducting materials either are not suited for these forms, do not exhibit properties better than the available technology, or are not feasible for economical reasons. This thesis will not be concerned with the hundreds of materials, but will focus on the technological ones.

The HTSC materials are able to work in temperatures above the boiling point of N (77K). The most notable of these are $Bi_2Sr_2CaCu_2O_{8-x}$ (Bi-2212), $(Bi,Pb)_2Sr_2Ca_2Cu_3O_{10-x}$ (Bi-2223) and $YBa_2Cu_3O_7$ (YBCO). They have T_cs of ~90 K, ~110 K and ~92 K respectively and at low temperatures all have H_{c2} values greater than 50 T [43, 44]. The major drawback of these HTSC materials is the difficulty of manufacturing them into useful forms. They have high H_{c2} anisotropy with parameters ($\gamma = H_{c2}^{\parallel}/H_{c2}^{\perp}$) above 20 and they also suffer from poor grain boundary connectivity. This means that they cannot be easily drawn into long length wires like the low T_c superconductors. They are usually made into tapes and have to be crystallographically textured to produce conductors with sufficiently high J_c for applications. These factors make them expensive to use.

Nb is one of the few elemental type-II superconductors and two of its alloys, NbTi and Nb_3Sn, are the most widely used in superconductor applications. NbTi wires are easy to make as the material in strong and ductile. Long lengths of multifilament wires can be inexpensively with high critical current densities. It has a transition temperature of ~9K and H_{c2} ~10-12K at 4.2K (liquid He) [43, 45]. More careful methods are needed to make Nb_3Sn wires as it is brittle and sensitive to strain. Nb_3Sn has T_c of 18K and H_{c2} of 23-29T at 4.2K [43, 46-49]. The difficulty in making and winding Nb_3Sn wires makes these magnets more expensive than NbTi. These two materials are classified as low temperature superconductors (LTS) and require cryogenic liquid helium to cool them during operation.

MgB_2 has a higher transition temperature than the niobium alloys. It is four times the T_c of NbTi and double the T_c of Nb_3Sn. MgB_2 is also capable of carrying a similar critical current density (J_c). It also has the advantage of well connected grains. It has moderate anisotropy (γ ~ 2-5) [2, 50] unlike the Nb alloys which can be considered isotropic but not as problematic as that of the HTSCs. Superconductors are used mainly for high field electromagnets and so are required to carry currents in high fields. Pure MgB_2 has $H_{c2}^{\parallel}$= 18T and $H_{c2}^{\perp}$ 3.5T, respectively, with fields parallel and perpendicular to the ab plane [50-54]. This poor performance at high fields is the main obstacle to the widespread use of MgB_2. It has been shown that the H_{c2} of MgB_2 can be hugely improved by introducing impurities that cause scattering [43]. This information has lead to numerous studies done on introducing scattering through doping and neutron irradiation. It is also the motivation for the work presented in this paper. The advantages of the various methods of increasing H_{c2} as well as the problems involved are discussed in a later section of this paper.

2.4. Fabrication of MgB_2 for magnets

Soon after the superconducting properties of MgB_2 were discovered it was found that good quality samples of pure MgB_2 were easy to synthesize by Mg diffusion into solid B. Sintered pellets were made by sintering commercially available Mg and B placed in Ta capsules and then in secondary containment [36, 55]. The samples made via this simple synthesis procedure were used to study the boron isotope effect [36] and later on revealed the transparency of MgB_2 grain boundaries to supercurrent flow [55]. The first MgB_2 wires were also made by this diffusion process [56]. Boron filaments with a tungsten core were sealed in a Ta tube which was then sealed in quartz and sintered at 950˚C. This process produced 80% dense wires with full Meissner state shielding. Single crystals have been made of MgB_2 to provide detailed information about the anisotropy of critical fields and currents [50, 51]. Thin films can be made by sputtering, CVD and PLD. The best superconducting MgB_2 samples to date are in the form of thin films, with reported values of $H_{c2} \sim 39$ T , $J_c(1T) \sim 10^6$ and $J_c(10T) \sim 10^5$ with a T_c of 31-36K [2, 11, 57, 58].

Since superconductors are mainly used in magnets, emphasis is placed on making long lengths of wire. Superconducting wires are generally composite conductors with a superconducting core and a sheath made of a suitable metal. The sheath material plays a few key roles. It mechanically supports the superconductor which is usually brittle, it conducts thermal energy out to the cryogen during operation and in the case of MgB_2 it contains the volatile Mg during sintering. The sheath material chosen must therefore be ductile, chemically compatible and it must be a good thermal conductor. Multifilament wires are preferable because they can endure larger bending strains than monofilaments. The small diameters for the superconductors achieved in multifilament wires also lead to better thermal stability. The PIT (powder in tube) method is a common process used for making composite multifilament MgB_2 wires. In this process the precursor is in powder form and placed into a tube of a suitable sheath material. The tube is then drawn into a wire and sintered. The process can be carried out either in-situ, where the powders are reacted after being drawn into wires, or ex-situ, where already reacted powders are inserted into the tube before drawing. The in-situ process is preferred because it allows lower sintering temperature and a more controllable way to add dopants [44]. Hyper Tech Research has patented a modified PIT process called continuous tube forming/filling (CTFF) [27]. In this process the precursor is deposited on a strip of sheath material as

it is being formed into an overlap-closed tube. This allows for continuous formation of powder filled tube and thus continuous lengths of drawn filaments. Hyper Tech uses Nb as a reaction barrier and Cu and Cu-Ni alloys as sheath materials. Using this process, 0.8mm diameter wires have been made in up to 5 km lengths and there is ongoing research to make wires up to 30 km long. It is highly desirable to develop means of synthesizing suitably doped MgB_2 powder with high values of H_{c2} for use in ex situ processing methods or appropriate mixtures of precursor powders from which suitably-doped MgB_2 is formed during in situ processing methods. This is the goal of the work described in this thesis.

2.5. Improving H_{c2} – impurity scattering

In type-II superconductors the H_{c2} value is directly related to the coherence length ξ according to Eq 2.4. The effective value of ξ of a doped or imperfect material is given by

$$\frac{1}{\xi} = \frac{1}{\xi_0} + \frac{1}{l} \qquad \text{Eq 2.7}$$

where ξ_0 is the coherence length of the pure material and l is the electron mean free path. If $l << \xi_0$ the actual ξ becomes l and if $\xi_0 << l$ it becomes ξ_0. The pure material coherence length is a constant of the material but the electron mean free path will become shorter with an increase in electron scattering. In a physical sense, the decreased ξ means that the diameter of the normal state flux line cores is smaller. So when a field is applied the material is able to contain more flux quanta without the overlapping of flux lines and thus the material can withstand a larger applied field. Researchers have taken advantage of this to increase the value of H_{c2} for superconducting materials.

Creating disorder by irradiation with protons [59, 60] as well as neutrons [61, 62] and ball milling [63, 64] have all proven to increase H_{c2}. These techniques cause damage and increase disorder and hence increase scattering. The other commonly used method is doping the sample with impurities. This has been used to improve H_{c2} in the LTS and HTSC materials superconductors in the past and has shown potential in MgB_2. Elements used in doping of MgB_2 include Sc and Al [65-68]which substitute for Mg in the lattice and C which replaces B [18, 69-71]. The major

drawback to all these reported experiments is the suppression of T_c with increases in scattering. This occurs because of interband scattering factors unique to the multiband MgB_2 and, in the case of doping, addition of electrons or electron-holes which alter the density of states and the electron-phonon interactions. Carbon is the most promising of the chemical substitutions because of the dominant contribution of the B orbitals to the superconductivity of MgB_2, especially in the σ band which is confined to the boron ab plane. The work presented in this paper deals with issues surrounding the carbon doping of MgB_2.

2.6. Carbon doping- reactions, homogeneity and precursors

Common reactions that produce high-quality samples of homogeneous MgB_2 do not result in the same homogeneity for C doped samples. In attempts to optimize this process carbon has been introduced by different means. These include the addition of SiC [72], nanoscale carbon [73], boron carbide (B_4C) [69] and hydrocarbons like toluene and acetone [74] as well as the ball milling of precursor powders [64]. It usually requires high reaction temperature and long reactions to get all the added C into the MgB_2 phase. This limits the ability to manipulate the microstructure of the superconductor for optimization of J_c and thermal stability. It is advantageous to create MgB_2 with small grain sizes as the grain boundaries are important for flux pinning and preventing flux creep. Also fluctuating microstrains in the lattice that provides additional scattering are relieved in long, hot reactions. Another concern is the grain to grain homogeneity of dopant levels. The most common B-C phase is B_4C and this has been used frequently as a precursor for MgB_2 synthesis. However this phase has a broad range of carbon concentration ranging from 7% to 20%. Dopant concentration in MgB_2 is usually indicated by the value of x in the formula $Mg(B_{1-x}C_x)_2$. The predicted optimal value of x is ~0.07 [69, 75] above which the gradient dH_{c2}/dx becomes negative. Therefore in a polycrystalline superconducting wire the measured critical fields and currents may be influenced by "weak" grains and not a true result of the average dopant concentration. Since the replacement of B by C in the crystal alters its average dimensions the lattice parameter, in particular that within the *ab* plane, the a parameter, as obtained from measured x-ray diffraction (XRD) spectra, is used as an indicator of x in a sample. Data from a systematic study on doped single crystal MgB_2 [18] have been fitted to produce the relationship [64]

$$a = -0.3153x + 3.08439 \quad \text{Eq 2.8}$$

between the boron plane lattice parameter a and the concentration of carbon, x. The C addition has the effect of reducing a with little or no effect on the lattice parameter c w, which characterizes the spacing between ab planes. The problem of homogeneity was investigated by Zambano et al [76] using the breadth , as characterized by the full width at half-maximum (FWHM) of the XRD peaks to calculate the residual root-mean-square microstrain which yields an estimate of the level of homogeneity of the doped sample.

The work in this thesis presents a unique method of preparing atomically mixed, nanoscale powders of B and C which are reacted with Mg to form C doped MgB_2. The small particle size and atomic mixing of elements is expected to aid in the production of homogeneously doped samples. The unique method of powder synthesis also results in metastable phases of B and C which could have further effects on the resulting superconductor.

3. Experimental Details

This experiment utilizes a unique fabrication process to synthesize nano-scale powder of carbon doped boron at the Center for Thermal Spray Research at Stony Brook University. Plasma spray is a thermal spray process that uses a hot plasma flame to melt and accelerate particles toward a substrate where they solidify upon impact. This process is usually employed to deposit functional coatings of alloys and ceramics on a substrate. In this process the raw materials are injected into a plasma torch which uses RF induction to create a dense plasma. The internal temperature of the plasma can exceed 10,000 ˚C. The powder synthesis process employed here is described by Marzik et al [77]. In this use of plasma spray the material is sprayed into a controlled chamber (~300Torr) where it solidifies. The torch used was a Tekna PL-50 and Ar was used as a sheath gas with a swirl flow ~30 standard liters per minute (SLPM) and a radial flow of ~70 SLPM.

The reactants inserted into the plasma were BCl_3, H_2 and CH_4. To ensure atomic mixing of the elements the reactants were all introduced in the gas phase with average flow rates of 5 SLPM, 12 SLPM and 0.100 SLPM respectively. When the gas mixture is exposed to the plasma the HCl and a B-C phase solidifies. The waste gas was pumped out through a water seal and the B-C powder was collected on a stainless steel screen. The particle size of the powder ranges from 2 to 50 nm and agglomerates into clusters that range from 1 to 50 μm in size. The powders used in this experiment had a molar C composition of 4.52% with B.

This B-C powders made in this way have advantageous features for the synthesis of C doped MgB_2. The atomic mixing and the small particle size should assist in the homogeneity of the final C concentration. The powders are processed in violently with extreme temperature and rapid solidification. This quenches the powder in metastable phases of B and C which eliminates the variation of composition of the stable phase B_4C and may prove to have an effect on the formation of the MgB_2 phase.

The powder described above is mixed with 325 mesh Mg powder from Alpha Aesar. Mg was added in excess of stoichiometry to account for losses due to its high vapor pressure. The mixture was then pressed into 6mm diameter pellets which were then wrapped in Ta foil and sealed in a stainless steel tube fitting. The samples were reacted at temperatures and times spanning those commonly used for MgB_2 synthesis. The samples and reaction parameters are listed in Table 1. The reacted samples were brittle and a dull grayish-black color. Each sample was cut into 1 mm x 1 mm x 10 mm bars used for resistive measurements taken at the National High Magnetic Field

Laboratory at Florida State University. The remaining sample was crushed and used for powder x-ray diffraction.

Sample	Reaction Time (hrs)	Sintering Temperature (˚C)
A	48	650
B	24	750
C	10	850
D	1	950
E	1	1050
F	1	1150

Table 3.1 Reaction parameters for samples A-F

4. Results and Discussion

4.1. X-ray Diffraction

The x-ray diffraction (XRD) patterns, shown in Figure 4.1, reveal a dominant MgB_2 phase and trace amounts of impurity phases. The presence of the impurity phases is most likely due to incomplete reaction due to loss of Mg or contamination from the stainless steel vessel. The peak shift due to carbon substitution was the same in all samples. The lattice parameter a as calculated by a least squares fit of the peak positions was used in Eq 2.8. The results showed good agreement with the full uptake of the nominal carbon (~5%) present during reaction. The small differences lie within the estimated margin of error. However, since the all the differences showed a composition greater than the nominal this indicates that the C concentration in the plasma-sprayed powder may be higher than expected. Table 4.1 lists all the lattice parameter data. Evidently, the plasma-sprayed powder allows full incorporation of the carbon regardless of the heat treatment temperature.

A method for studying the homogeneity of the substitution of carbon for boron is the analysis of the residual strain as suggested by Zambano et al [76]. By using the Williamson-Hall (WH) method [78] one can differentiate the peak broadening effects of the grain size and strain, the latter presumably resulting from an inhomogeneous distribution of C. The breadth of the reciprocal lattice points (β*) and their distance from the origin (d*) are calculated from the full width at half maximum (W) of the peaks and the Bragg angle (θ)

$$\beta^* = \frac{W \cos\theta}{\lambda} \qquad \text{Eq 4.1}$$

$$d^* = \frac{2 \sin\theta}{\lambda} \qquad \text{Eq 4.2}$$

where λ is the wavelength of the x-rays and is 1.5418 Å for the Cu source used. Then β* is plotted against d*. These quantites are related by

$$\beta^* = \frac{1}{D} + \frac{\varepsilon}{2} d^* \qquad \text{Eq 4.3}$$

where D is the effective grain size and ε is the root-mean-square (rms) average of the fluctuating strain throughout a coherently-diffracting domain. Thus the plot of β* versus d* has slope of ε/2 and intercepts the vertical axis at 1/D. The four Bragg reflections used are (100), (101), (110) and (201). The effect of C addition in the MgB_2 lattice is to decrease the *a* parameter with little or no effect on the *c* parameter. The fact that the *a* parameter is affected by the C content while the *c* parameter is not means that the (hk0) peaks will have more broadening than the (hk1) peaks and a linear fit of all four points is not expected. The strains are therefore analyzed by connecting two (hk0) data points with a straight line and likewise for the (hk1) points. The WH plots for samples A-F are given in Figure 4.2. The WH plots for pure MgB_2 found in the literature show a residual strain close to 0.4% [76]. In this case the rms-microstrains are presumably caused by dislocations, stacking faults and other crystal structure defects rater than inhomogeneously distributed solute atoms.

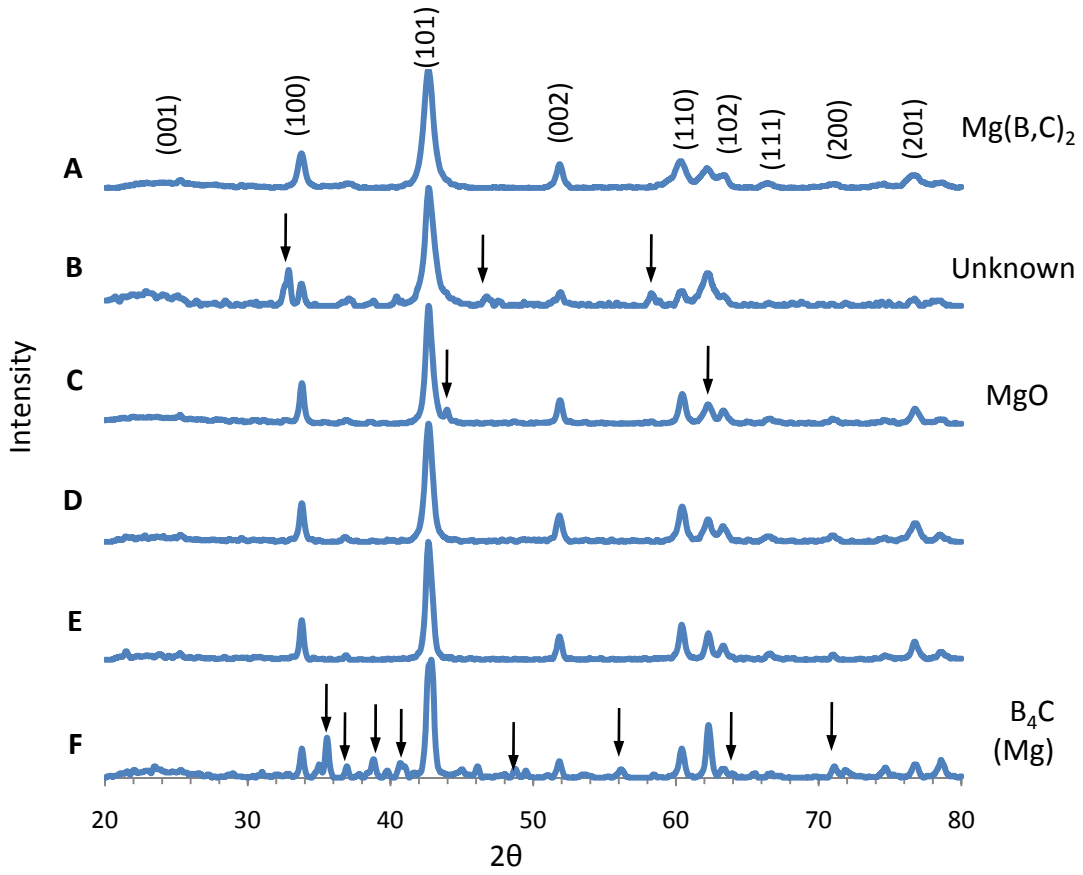

Figure 4.1 X-ray diffraction data are shown for samples A-F. The spectra have been offset to provide clarity. The peak positions for the MgB_2 phase are indicated in the spectra for sample A and other impurity phases are labeled in the spectra they appear the strongest.

Sample	*a* (Å)	*C* (Å)	*Nominal x*	*Calculated X*
A	3.068(5)	3.526(6)	0.045	0.052
B	3.066(5)	3.525(5)	0.045	0.058
C	3.065(5)	3.528(5)	0.045	0.061
D	3.065(5)	3.531(5)	0.045	0.061
E	3.066(5)	3.531(5)	0.045	0.058
F	3.065(6)	3.529(7)	0.045	0.061

Table 4.1 Lattice parameters a and c from the peak positions in XRD spectra. The nominal C concentration x and the calculated x (Eq 2.8) are also listed.

The data, especially the (201) data, are slightly scattered but the data sets show a slightly greater strain than 0.4%. However, this is much lower than the massive strains seen in similarly sintered Al-doped [76] that were caused by large concentration gradients of the alloying element. The WH plots give evidence to the homogeneous alloying that results from the plasma spray precursor. The (hk0) plots display a trend of decreasing strain with increasing reaction temperature below 950˚C. This trend is not seen in the pure material data and could be a feature of disorder which is reduced by annealing at high temperatures. Moreover, the XRD patterns show presence of the B-C equilibrium phase B_4C in sample F. Since the B-C precursor is nanoscale and has low atomic mass elements, any unreacted B and C would not give sharp peaks but would contribute to the "hump" seen at low angles. This B and C form crystalline B_4C when annealed at high temperature.

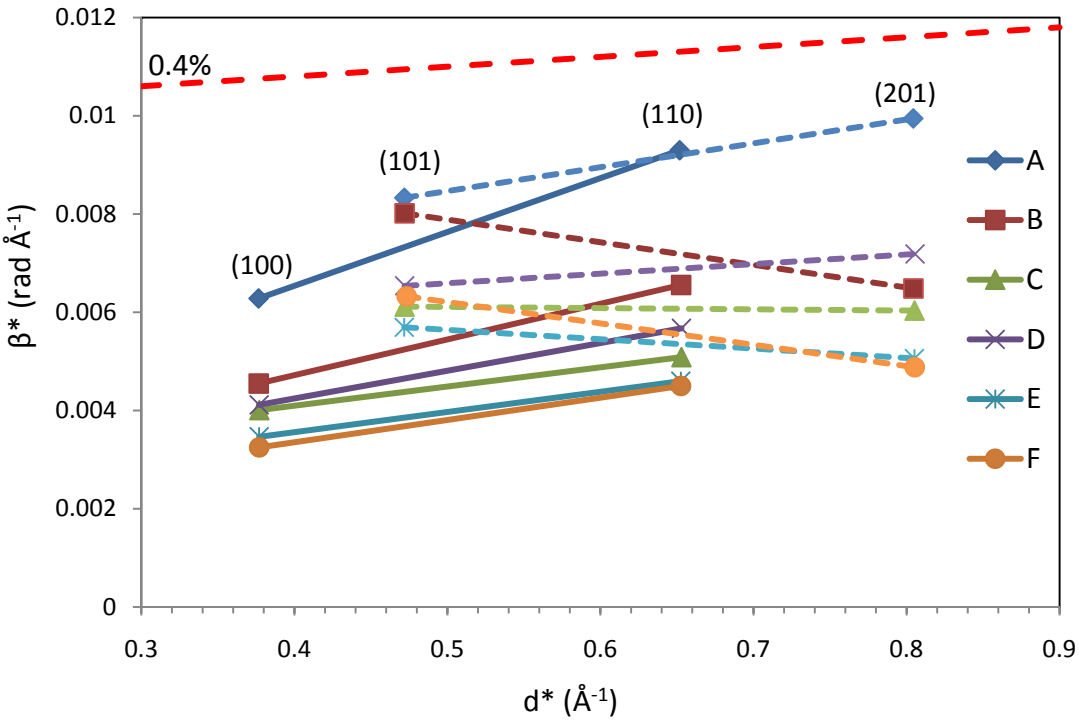

Figure 4.2 Williamson-Hall plots are shown for samples A-F. The samples and the diffraction peaks are indicated on the plot. The red dashed line to the top shows ε = 0.004 for comparison.

4.2. Resistivity Measurements

The resistivity of the 1 mm x 1mm x 10 mm bars was measured while being cooled from 300 K to 20 K in self field. All samples showed sharp transitions between 33 K and 29 K with transition widths ranging from 2 to 5 K. The presence of carbon and other imperfections in known to reduce T_c. The difference in T_c here is small and could be explained by a slightly increased amount of carbon in the MgB_2 phase (as evidenced in the lattice parameter analysis) when annealed at high temperature. The T_c data is shown in Figure 4.3. The range of T_cs obtained is in good agreement with similar dopant concentrations in single crystal data [18] and with the XRD data given above, which also suggests low levels of interband scattering unlike the ball-milled material [64].

The H_{c2} measurements were taken at varying temperatures and up to 9 T. The H_{c2} values are plotted against temperature in Figure 4.4. The trend observed is the same as the T_c where higher reaction temperatures lead to lower H_{c2}. A linear extrapolation gives H_{c2} at 0 K to be ~32 T for the best sample. The elevated H_{c2} values are excellent for the incorporated carbon content especially in sample A which was reacted at the lowest temperature. The slope dH_{c2}/dT does not increase, but instead the entire curves shift upward which is consistent with constant alloying and resistivty.

The H_{c2} of a dirty superconductor is related to the T_c and normal state resistivity (ρ_n) by the Werthamer-Helfand-Hohenburg (WHH) equation

$$H_{c2}(0\text{K}) = 3110\rho_n\gamma T_c \qquad \text{Eq 4.4}$$

where γ is the Somerfield coefficient of specific heat and can be considered constant in this case. The addition of impurities affects both ρ_n and T_c. In the case of carbon substitution in MgB_2 the effect of the T_c is due to the lattice parameter shift and the additional electrons affecting the density of states. The balancing act of increasing ρ_n and reducing T_c is seen in the data from these samples. The B-C powder used in this experiment has potential of significantly increasing the high field performance in MgB_2 in the 20-30 K range.

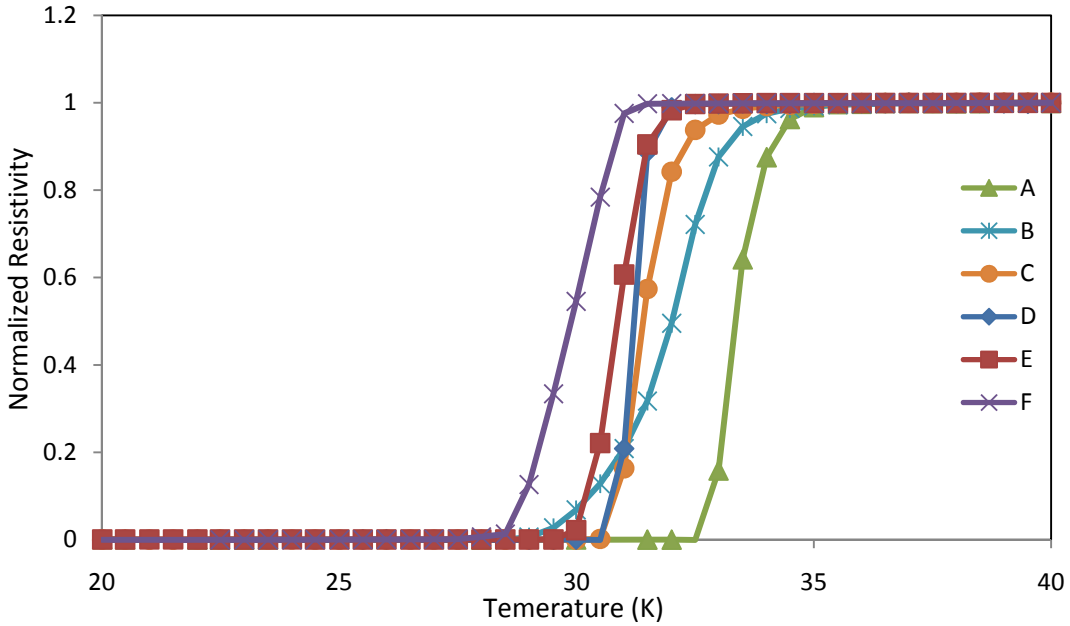

Figure 4.3 The superconducting transitions at self field for samples A-F. The resistivity is normalized to aid comparison of the transition temperatures.

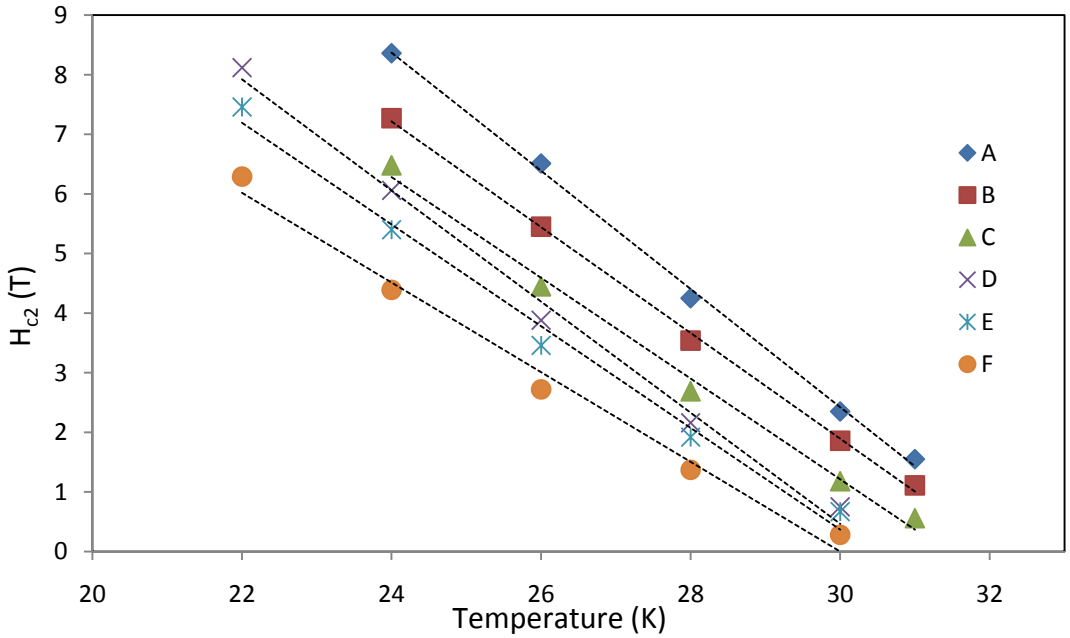

Figure 4.4 H_{c2} versus T for samples A-F. The straight line fit for all plots are shown by dotted lines.

Using the Rowell analysis [79] of the normal state resistivity of MgB_2 allows the normalization of the resistivity in terms of the area fraction of superconductor. This is useful to compare the superconducting material made in different reactions. The results of this analysis on samples A through F gave inconsistent results over a few orders of magnitude. This is most likely a result of the porosity and cracking from mechanical stress during sample preparation and the impurity phases seen in the XRD spectra. The preferred method of sintering is by using an isostatic hot press. This would ensure dense material and well connected grains by applying pressure throughout the reaction. This was attempted but was not successful due to equipment malfunction. The residual resistivity ratio (RRR) defined as $\rho(300\ K)/\ \rho(40\ K)$ was similar for all samples. This is another indicator of the ability to consistently add carbon at different temperatures using the plasma-sprayed powder.

5. Conclusion

The plasma spray synthesis of carbon doped boron provides a unique avenue for the production of high field superconducting MgB_2. The combination of gaseous reactants, high temperature and rapid solidification provides a nanoscale powder containing metastable phases of B and C. The microstrain, lattice parameter, critical temperature and normal state resistivity measurements are all consistent with uniform incorporation of carbon at all reaction temperatures. The results for samples sintered at low temperatures are particularly desirable for wire fabrication. This method of carbon doping has potential to make MgB_2 the preferred superconductor for high – field applications in the 20-30 K range. The precursor powder can be used for both *in situ* and *ex situ* PIT processes, including the CTFF process used by Hyper Tech Research. The attributes of this doping method can also provide insight into the multiband effects in MgB_2 and possibly additional means of improving its high field performance.

There are still more studies to be done on this process in order to achieve the full scale use of MgB_2 wires. The plasma spray powder should be studied to understand phase composition created during the plasma spray process. This may help in understanding the impurity phases that appear at high temperatures may block current and reduce the H_{c2} values of these samples and provide methods to reduce this effect. The nanoscale particle size and low elemental can be studied using electron energy loss spectroscopy and synchrotron light source radiation. The sintering process needs improvement to made dense, well-connected samples for more quantifiable superconducting property data.

Bibliography

1. Nagamatsu, J., et al., *Superconductivity at 39 K in magnesium diboride.* Nature, 2001. **410**(6824): p. 63-64.

2. Buzea, C. and T. Yamashita, *Review of the superconducting properties of MgB2.* Superconductor Science & Technology, 2001. **14**(11): p. R115-R146.

3. da Silva, R.R., J.H.S. Torres, and Y. Kopelevich, *Indication of Superconductivity at 35 K in Graphite-Sulfur Composites.* Physical Review Letters, 2001. **87**(14): p. 147001.

4. Young, D.P., et al., *Superconducting properties of BeB2.75.* Physical Review B, 2002. **65**(18): p. 180518.

5. Gasparov, V.A., et al., *Electron transport in diborides: Observation of superconductivity in ZrB2.* Jetp Letters, 2001. **73**(10): p. 532-535.

6. He, T., et al., *Superconductivity in the non-oxide perovskite MgCNi3.* Nature, 2001. **411**(6833): p. 54-56.

7. Eremets, M.I., et al., *Superconductivity in Boron.* Science, 2001. **293**(5528): p. 272-274.

8. Dai, P., et al., *Synthesis and neutron powder diffraction study of the superconductor HgBa2Ca2Cu3O8+delta by Tl substitution.* Physica C, 1995. **243**(3-4): p. 201-206.

9. Ferdeghini, C., et al., *Some aspects of material preparation in magnesium diboride: Thin films growth and tapes fabrication.* International Journal of Modern Physics B, 2003. **17**(4-6): p. 400-406.

10. Grassano, G., et al., *As-grown magnesium diboride superconducting thin films deposited by pulsed laser deposition.* Superconductor Science & Technology, 2001. **14**(9): p. 762-764.

11. Ivanov, Z., et al., *Superconductivity in magnesium diboride thin films.* Physica C-Superconductivity and Its Applications, 2002. **372**: p. 1274-1276.

12. Ma, P., et al., *Single-step in-situ preparation of magnesium diboride superconducting thin films by dc magnetron sputtering.* Acta Physica Sinica, 2002. **51**(2): p. 406-409.

13. Rowell, J., *Magnesium diboride - Superior thin films.* Nature Materials, 2002. **1**(1): p. 5-6.

14. Uchiyama, T., H. Koga, and I. Iguchi, *Novel preparation method for superconducting magnesium-diboride thin films with high-T-c.* Physica C-Superconductivity and Its Applications, 2004. **412**: p. 1362-1365.

15. Kim, K.H.P., et al., *Superconducting properties of well-shaped MgB2 single crystals.* Physical Review B, 2002. **65**(10).

16. Lee, S., et al., *Growth, structure analysis and anisotropic superconducting properties of MgB2 single crystals.* Journal of the Physical Society of Japan, 2001. **70**(8): p. 2255-2258.

17. Xu, M., et al., *Anisotropy of superconductivity from MgB2 single crystals.* Applied Physics Letters, 2001. **79**(17): p. 2779-2781.

18. Kazakov, S.M., et al., *Carbon substitution in MgB2 single crystals: Structural and superconducting properties.* Physical Review B, 2005. **71**.

19. Bhatia, M., et al., *Influence of heat-treatment schedules on the transport current densities of long and short segments of superconducting MgB2 wire.* Physica C: Superconductivity, 2004. **407**(3-4): p. 153-159.

20. Braccini, V., et al., *Development of ex situ processed MgB2 wires and their applications to magnets.* Physica C: Superconductivity, 2007. **456**(1-2): p. 209-217.

21. Suo, H.L., et al., *Transport critical current densities and n factors in mono- and multifilamentary MgB2/Fe tapes and wires using fine powders.* Ieee Transactions on Applied Superconductivity, 2003. **13**(2): p. 3265-3268.

22. Tanaka, K., et al., *Fabrication and transport vroperties of MgB2/(SUS316/Cu) multifilament wires.* Ieee Transactions on Applied Superconductivity, 2004. **14**(2): p. 1039-1041.

23. Malagoli, A., et al., *Fabrication and superconducting properties of powder-in-tube processed MgB2 tapes.* Physica C: Superconductivity, 2002. **372-376**(Part 2): p. 1245-1247.

24. Li, X.H., et al. *Design and experimental demonstration of an MgB2 based 1.5 T MRI test magnet*. 2007: Elsevier Science Bv.

25. Serquis, A., et al., *Large field generation with a hot isostatically pressed powder-in-tube MgB2 coil at 25 K.* Superconductor Science & Technology, 2004. **17**(10): p. L35-L37.

26. *Press release*. 2006 [cited 2008 12-03]; Available from: http://www.columbussuperconductors.com/Press%20release.pdf.

27. Tomsic, M., et al., *Overview of MgB2 superconductor applications.* International Journal of Applied Ceramic Technology, 2007. **4**(3): p. 250-259.

28. Ivanovskii, A.L., *Band structure and properties of superconducting MgB2 and related compounds (a review).* Physics of the Solid State, 2003. **45**(10): p. 1829-1859.

29. Souma, S., et al., *The origin of multiple superconducting gaps in MgB2.* Nature, 2003. **423**(6935): p. 65-67.

30. Bouquet, F., et al., *Specific heat of (MgB2)-B-11: Evidence for a second energy cap.* Physical Review Letters, 2001. **8704**(4): p. 4.

31. Chen, X.K., et al., *Evidence for two superconducting gaps in MgB2.* Physical Review Letters, 2001. **8715**(15): p. 4.

32. Choi, H.J., et al., *The origin of the anomalous superconducting properties of MgB2.* Nature, 2002. **418**(6899): p. 758-760.

33. Bardeen, J., L.N. Cooper, and J.R. Schrieffer, *MICROSCOPIC THEORY OF SUPERCONDUCTIVITY.* Physical Review, 1957. **106**(1): p. 162-164.

34. Richardson, C.F. and N.W. Ashcroft, *High temperature superconductivity in metallic hydrogen: Electron-electron enhancements.* Physical Review Letters, 1997. **78**(1): p. 118-121.

35. Yildirim, T., et al., *Giant anharmonicity and nonlinear electron-phonon coupling in MgB2: A combined first-principles calculation and neutron scattering study.* Physical Review Letters, 2001. **8703**(3): p. 4.

36. Bud'ko, S.L., et al., *Boron isotope effect in superconducting MgB2.* Physical Review Letters, 2001. **86**(9): p. 1877-1880.

37. Cooper, L.N., *BOUND ELECTRON PAIRS IN A DEGENERATE FERMI GAS.* Physical Review, 1956. **104**(4): p. 1189-1190.

38. Pines, D., *Superconductivity in the Periodic System.* Physical Review, 1958. **109**(2): p. 280.

39. Maxwell, E., *Isotope Effect in the Superconductivity of Mercury.* Physical Review, 1950. **78**(4): p. 477.

40. Reynolds, C.A., et al., *Superconductivity of Isotopes of Mercury.* Physical Review, 1950. **78**(4): p. 487.

41. Brotto, P., et al., *Experimental confirmation of the low B isotope coefficient of MgB2.* Physical Review B, 2008. **78**(9): p. 4.

42. Hinks, D.G., H. Claus, and J.D. Jorgensen, *The complex nature of superconductivity in MgB2 as revealed by the reduced total isotope effect.* Nature, 2001. **411**(6836): p. 457-460.

43. Gurevich, A., et al., *Very high upper critical fields in MgB2 produced by selective tuning of impurity scattering.* Superconductor Science and Technology, 2004(2): p. 278.

44. Vinod, K., R.G.A. Kumar, and U. Syamaprasad, *Prospects for MgB2 superconductors for magnet application.* Superconductor Science & Technology, 2007. **20**(1): p. R1-R13.

45. Zheng, D.N., N.J.C. Ingle, and A.M. Campbell, *Irreversibility fields of superconducting niobium alloys.* Physical Review B, 2000. **61**(22): p. 15429.

46. Cooley, L.D., Y.F. Hu, and A.R. Moodenbaugh, *Enhancement of the upper critical field of Nb[sub 3]Sn utilizing disorder introduced by ball milling the elements.* Applied Physics Letters, 2006. **88**(14): p. 142506-3.

47. Godeke, A., *A review of the properties of Nb3Sn and their variation with A15 composition, morphology and strain state.* Superconductor Science & Technology, 2006. **19**(8): p. R68-R80.

48. Godeke, A., et al., *The upper critical field of filamentary Nb3Sn conductors.* Journal of Applied Physics, 2005. **97**(9).

49. Suenaga, M., et al., *SUPERCONDUCTING CRITICAL-TEMPERATURES, CRITICAL MAGNETIC-FIELDS, LATTICE-PARAMETERS, AND CHEMICAL-COMPOSITIONS OF BULK PURE AND ALLOYED NB3SN PRODUCED BY THE BRONZE PROCESS.* Journal of Applied Physics, 1986. **59**(3): p. 840-853.

50. Angst, M., et al., *Temperature and Field Dependence of the Anisotropy of MgB2.* Physical Review Letters, 2002. **88**(16): p. 167004.

51. Perkins, G.K., et al., *Superconducting critical fields and anisotropy of a MgB2 single crystal.* Superconductor Science and Technology, 2002(7): p. 1156.

52. Sologubenko, A.V., et al., *Temperature dependence and anisotropy of the bulk upper critical field Hc2 of MgB2.* Physical Review B, 2002. **65**(18): p. 180505.

53. Zehetmayer, M., et al., *Mixed-state properties of superconducting MgB2 single crystals.* Physical Review B, 2002. **66**(5): p. 052505.

54. Canfield, P.C., S.L. Bud'ko, and D.K. Finnemore, *An overview of the basic physical properties of MgB2.* Physica C-Superconductivity and Its Applications, 2003. **385**(1-2): p. 1-7.

55. Larbalestier, D.C., et al., *Strongly linked current flow in polycrystalline forms of the superconductor MgB2.* Nature, 2001. **410**(6825): p. 186-189.

56. Canfield, P.C., et al., *Superconductivity in Dense MgB2 Wires.* Physical Review Letters, 2001. **86**(11): p. 2423.

57. Patnaik, S., et al., *Electronic anisotropy, magnetic field-temperature phase diagram and their dependence on resistivity in c-axis oriented MgB2 thin films.* Superconductor Science and Technology, 2001(6): p. 315.

58. Eom, C.B., et al., *High critical current density and enhanced irreversibility field in superconducting MgB2 thin films.* Nature, 2001. **411**(6837): p. 558-560.

59. Gandikota, R., et al., *Effect of damage by 2 MeV He ions and annealing on H(c)2 in MgB2 thin films.* Applied Physics Letters, 2005. **87**(7).

60. Bugoslavsky, Y., et al., *Enhancement of the high-magnetic field critical current density of superconducting MgB2 by proton irradiation.* Nature, 2001. **411**(6837): p. 561-563.

61. Putti, M., et al., *Neutron irradiation of (MgB2)-B-11: From the enhancement to the suppression of superconducting properties.* Applied Physics Letters, 2005. **86**(11).

62. Eisterer, M., et al., *Neutron irradiation of MgB2 bulk superconductors.* Superconductor Science and Technology, 2002(2): p. L9.

63. Gumbel, A., et al., *Improved superconducting properties in nanocrystalline bulk MgB2.* Applied Physics Letters, 2002. **80**(15): p. 2725-2727.

64. Senkowicz, B.J., et al., *Improved upper critical field in bulk-form magnesium diboride by mechanical alloying with carbon.* Applied Physics Letters, 2005. **86**(20).

65. Slusky, J.S., et al., *Loss of superconductivity with the addition of Al to MgB2 and a structural transition in Mg1-xAlx.* Nature, 2001. **410**(6826): p. 343-345.

66. Luo, H., et al. *Study of Al doping effect on superconductivity of Mg1-xAlxB2*. 2002: Amer Inst Physics.

67. Postorino, P., et al., *Effect of the Al content on the optical phonon spectrum in Mg1-xAlxB2.* Physical Review B, 2002. **65**(2): p. 4.

68. Agrestini, S., et al., *Substitution of Sc for Mg in MgB2: Effects on transition temperature and Kohn anomaly.* Physical Review B, 2004. **70**(13): p. 5.

69. Wilke, R.H.T., et al., *Systematic effects of carbon doping on the superconducting properties of Mg(B1-xCx)(2).* Physical Review Letters, 2004. **92**(21): p. 4.

70. Ribeiro, R.A., et al., *Carbon doping of superconducting magnesium diboride.* Physica C-Superconductivity and Its Applications, 2003. **384**(3): p. 227-236.

71. Lee, S., et al., *Carbon-substituted MgB2 single crystals.* Physica C-Superconductivity and Its Applications, 2003. **397**(1-2): p. 7-13.

72. Wang, X.L., et al., *Significant improvement of critical current density in coated MgB2/Cu short tapes through nano-SiC doping and short-time in situ reaction.* Superconductor Science and Technology, 2004(3): p. L21.

73. Dou, S.X., et al., *Effect of carbon nanotube doping on critical current density of MgB2 superconductor.* Applied Physics Letters, 2003. **83**(24): p. 4996-4998.

74. Xu, X., et al., *Improved J(c) of MgB2 superconductor by ball milling using different media.* Superconductor Science & Technology, 2006. **19**(11): p. L47-L50.

75. Wilke, R.H.T., et al., *Synthesis of Mg(B1-xCx)(2) powders.* Physica C-Superconductivity and Its Applications, 2005. **432**(3-4): p. 193-205.

76. Zambano, A.J., A.R. Moodenbaugh, and L.D. Cooley, *Effects of different reactions on composition homogeneity and superconducting properties of Al-doped MgB/sub 2.* Superconductor Science & Technology, 2005. **18**(11): p. 1411-1420.

77. Marzik, J.V., et al., *Plasma synthesized doped B powders for MgB2 superconductors.* Physica C-Superconductivity and Its Applications, 2005. **423**(3-4): p. 83-88.

78. Williamson, G.K. and W.H. Hall, *X-ray line broadening from filed aluminium and wolfram.* Acta Metallurgica, 1953. **1**(1): p. 22-31.

79. Rowell, J.M., *The widely variable resistivity of MgB2 samples.* Superconductor Science & Technology, 2003. **16**(6): p. R17-R27.